Polymer(Korea), Vol. 41, No. 1, pp. 68-74 (2017)
https://doi.org/10.7317/pk.2017.41.1.68

ISSN 0379-153X(Print)
ISSN 2234-8077(Online)

초고분자량 폴리에틸렌 그래핀옥사이드 강화복합체의 제조 및 트라이볼로지 특성연구

Xinjun Hu, Xiaojie Yan, Yu Ma, and Yongxiao Bai†

Key Laboratory for Magnetism and Magnetic Materials, Institute of Material Science and Engineering, Lanzhou University

(2016년 6월 28일 접수, 2016년 8월 18일 수정, 2016년 8월 29일 채택)

Synthesis and Tribological Performance Study of Ultrahigh Molecular Weight Polyethylene Composites Reinforced with Graphene Oxide

Xinjun Hu, Xiaojie Yan, Yu Ma, and Yongxiao Bai†

Key Laboratory for Magnetism and Magnetic Materials, Institute of Material Science and Engineering, Lanzhou University, Lanzhou 730000, China

(Received June 28, 2016; Revised August 18, 2016; Accepted August 29, 2016)

Abstract: In order to improve the hardness and tribological properties of ultrahigh molecular weight polyethylene (UHMWPE), UHMWPE composites reinforced with graphene oxide (GO) nanosheets by ball milling is presented in this article. The results show that the content of 20 wt% GO composite exhibits the lowest friction coefficient and the best wear resistance among all specimens under distilled water lubrication conditions. The mechanism of GO content on tribological properties of the composites under dry conditions and distilled water were investigated. Super low friction coefficient value and the best wear resistance under distilled water is attributed to water provides passivation of interacting dangling bonds on the sliding surface of GO. This study provides a new path to synthesize the high wear resistance and mechanical performance GO/UHMWPE composite materials under water condition and may have huge potential applications in many related fields, such as biomedical and marine engineering.

Keywords: nanocomposites, UHMWPE, graphene oxide, wear and friction, hardness.

Introduction

Ultrahigh molecular weight polyethylene (UHMWPE) is a unique polymer with outstanding physical and mechanical properties, which display excellent bio-compatibility, chemical stability, impact strength, high wear resistance and low friction. These characteristics of UHMWPE have been exploited since the 1950s in a wide range of industrial applications, including pickers for textile machinery, lining for coal chutes and dump trucks, runners for bottling production lines, as well as bumpers and siding for ships and harbors. However, UHMWPE has some disadvantages: its hardness and Young's modulus are low, and it easily creeps under load. This restricts its load-bearing capacity.[1]

In order to improve the mechanical and tribological properties of UHMWPE, kaolin, alumina, zirconium and carbon-based fillers have been used as reinforcing filler materials.[2-5] Graphene is one-atom-thick two-dimensional (2D) layers of sp2-bonded carbon atoms arranged in a honeycomb lattice. Since experimentally discovered in 2004 by K. S. Novoselov and A. K. Geim,[6] graphene has become one of most exciting research topics owing to its fascinating properties, such as giant electron mobility, extremely high thermal conductivity, extraordinary elasticity and stiffness, large surface area, high thermal stability, and low cost in compared with carbon nanotube (CNT).[7-9] Especially, the latest developments in tribological applications of graphene and theoretical simulations of graphene friction have shown that graphene is one of the ideal fillers in polymer composites, which can significantly improve the tribological performances of host polymer.[10-15]

In this paper, UHMWPE composites reinforced with graphene oxide (GO) nanosheets were prepared by ball milling,

†To whom correspondence should be addressed.
E-mail: baiyx@lzu.edu.cn

the effect of the GO content of the composites on the tribological properties in both dry and water lubrication conditions and hardness were also investigated. Moreover, the wear mechanisms of GO/UHMWPE composite were discussed.

Experimental

Materials. Graphite powder purchased from Sinopharm Chemical Reagent Co. Ltd (Shanghai, China), UHMWPE with an average molecular weight of 2.1×10^6 and a mean particle diameter of about 300 μm was supplied from lanzhou Petrochemical Co., Ltd., China. Other chemical reagents and solvents were from Tianjin Guangfu Fine Chemical Research Institute (Tianjin, China) and used directly without further purification.

Preparation of Graphite Oxide. Graphite oxide was synthesized from natural graphite powder by a modified Hummers method.[16-18] Typically, Graphite powder 12 g(45 μm) was put into an 85 °C solution of concentrated H_2SO_4 (48 mL), $K_2S_2O_8$ (10 g), and P_2O_5 (10 g). The mixture was kept at 80 °C for 4.5 h using a water bath. Successively, the mixture was cooled to room temperature and diluted with 2 L of de-ionized (DI) water. Then, the mixture was filtered and washed with de-ionized (DI) water to remove the residual acid. The product was dried under ambient condition. This pre-oxidized graphite was then subjected to oxidation by Hummers' method described as follows. Pretreated graphite powder was put into cold (0 °C) concentrated H_2SO_4 (460 mL). Then, $KMnO_4$ (60 g) was added gradually under stirring and the temperature of the mixture was kept to be below 20 °C by cooling. Successively, the mixture was stirred at 35 °C for 2 h, and then diluted with DI water (250 mL). Because the addition of water in concentrated sulfuric acid medium released a large amount of heat, the addition of water was carried out in an ice bath to keep the temperature below 50 °C. After adding all of the DI water, the mixture was stirred for 2 h, and then additional 2.8 L of DI water was added. Shortly after the dilution with 2.8 L of water, 80 mL of 30% $H_2O_2$was added to the mixture, and the color of mixture changed into brilliant yellow along with bubbling. For purification, the mixture was washed with a dilute hydrochloric acid solution (5%) and deionized water until the pH of the supernatant reached 6. The resulting graphite oxide powder was shortly dried in air.

Preparation of GO/UHMWPE Composite. Powders of graphite oxide were put into the solid state in a mechanical high energy ball mill (Fritsch Pulverisette 4) for 30 h at a speed of 250 rpm, then milled with the UHMWPE powder for 3 h at a speed of 250 rpm. Under these conditions, UHMWPE composites with 1, 5, 10, 15 and 20 wt% of GO were obtained. The pure UHMWPE and the UHMWPE composites were molded in a hot press at 200 °C for 30 min at 15 MPa pressure, obtaining a rectangular slice with the size of $40\times10\times6$ mm^3. For the wear tests, specimens were cut into $30\times7\times6$ mm^3.

Characterizations. The friction and wear behavior of the composites were test on a M-200 tester (Figure 1). The GO-filled UHMWPE block samples were loaded against 45 L stainless steel rings, with a rotating velocity of 200 rpm, i.e. the sliding velocity 0.42 m/s. The test was carried out under dry and distilled water lubrication conditions with 196 N normal loads for 2 h, respectively. Each test was repeated three times at least. The wear mass loss of the samples was determined by an electronic analytical balance with an accuracy of 0.1 mg, the wear traces of samples were examined by scanning electron microscopy (SEM; Hitachi S-4800). Typical tapping-mode atomic-force microscopy (AFM) measurements were performed using Multimode SPM from Digital Instruments with a Nanoscope IV Controller made by Asylum Research Inc. Samples for AFM images were prepared by depositing a dispersed GO solution onto a freshly cleaved mica surface. Differential scanning calorimetric (DSC) measurements were carried out under dry nitrogen using a DSC analyzer (Netzsch DSC 204 F1) from 40 to 270 °C at 10 °Cmin^{-1}. Thermogravimetric analysis (TGA) for the samples was performed on Perkin-Elmer Diamond thermal analyzer from room temperature to 600 °C. X-ray diffraction (XRD) patterns were recorded by a Rigaku D/Max-2400 diffractometer using Cu Kα radiation. The measurement of hardness was carried on a Shore hardness tester (CY-D; Suzhou Quantum Instruments Co., Ltd). For accuracy, at least six points were measured and the resulted values were averaged.

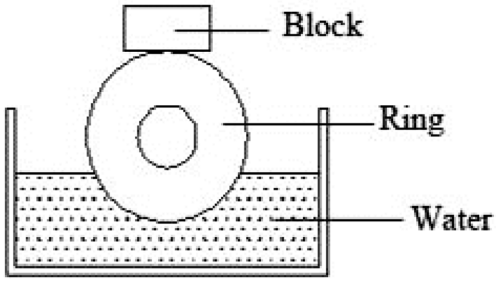

Figure 1. Contact mode of friction pair for wear tests.

Results and Discussion

AFM image (Figure 2(a)) of the hydrosol offers immediate evidence for peeled-off single GO sheets. The thicknesses of the graphene oxide layers we prepared are within a very narrow range of 1.1-1.2 nm, SEM image (Figure 2(b)) revealed most GO sheets had the lengths range of 1-3 μm. GO layers are somewhat larger than the interlayer spacing (0.776 nm) of the parent GO, due to the presence of oxygen-containing groups and the displacement of the sp3-hybridized carbon atoms slightly above and below the original graphene plane.[8]

XRD is an important tool for determining whether graphene-based sheets are indeed present as individual graphene sheets in the composites or not. Figure 3 shows the XRD pattern of GO reinforced UHMWPE composites with the amount of GO changed, the typical diffraction peak of GO was observed at about 10.4°.[19] However, after GO was dispersed into the UHMWPE matrix, the XRD pattern of the composites only showed the UHMWPE diffraction peak from UHMWPE and the diffraction peak of GO was disappeared. The XRD results clearly demonstrated that GO was fully exfoliated into individual GO sheets in the polymer matrix and that the regular and periodic structure of GO disappeared.[5,11,20] To investigate the surface morphology of the cross sections of the 20 wt% GO/UHMWPE composites, SEM images of the cross sections of composites were measured (Figure 4). A great amount of edges of GO were observed on the surface of GO/UHMWPE composite, indicating GO were well dispersed in the composite.

Figure 5 shows the influence of the GO wt% in UHMWPE composites on the friction coefficient with sliding time within

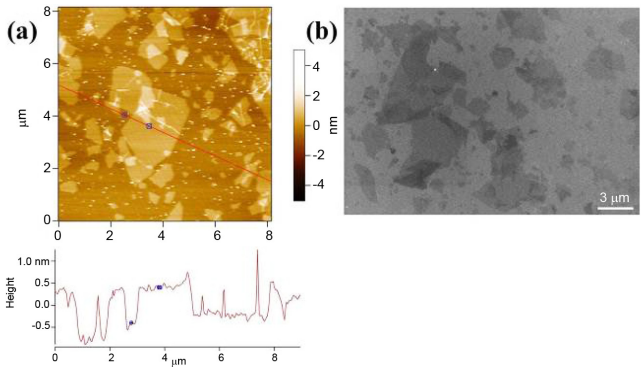

Figure 2. (a) Typical tapping-mode AFM image of GO deposited on mica substrate; (b) SEM image of GO sheets deposited on the rinsed silicon wafer.

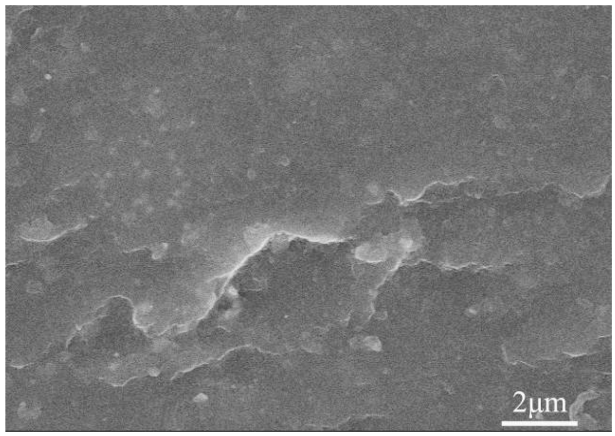

Figure 4. SEM image of the cross section of 20 wt% GO/UHMWPE composites.

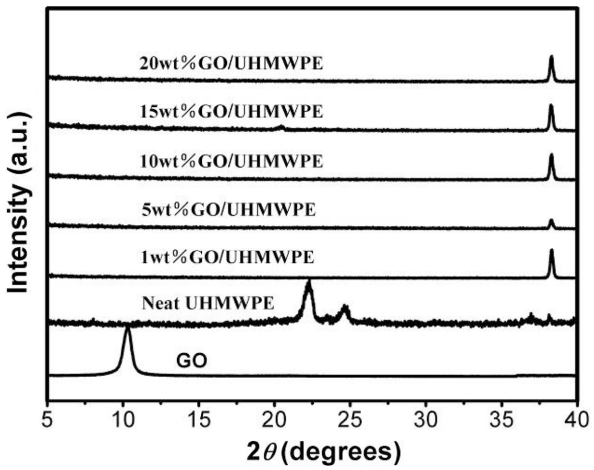

Figure 3. XRD pattern of GO reinforced UHMWPE composites with the amount of GO changed.

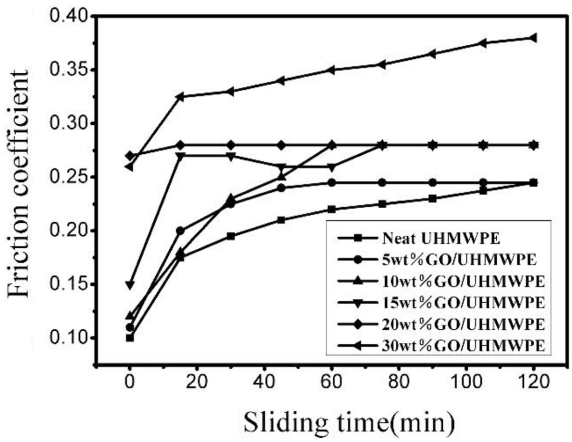

Figure 5. Influence of the GO wt% in UHMWPE composites on the friction coefficient under dry condition.

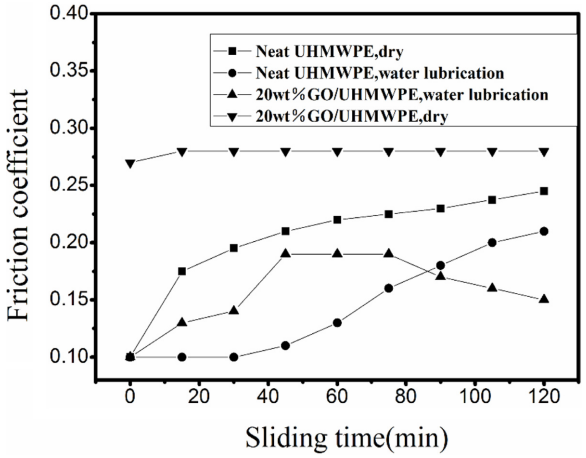

Figure 6. Variation of friction coefficient with sliding time.

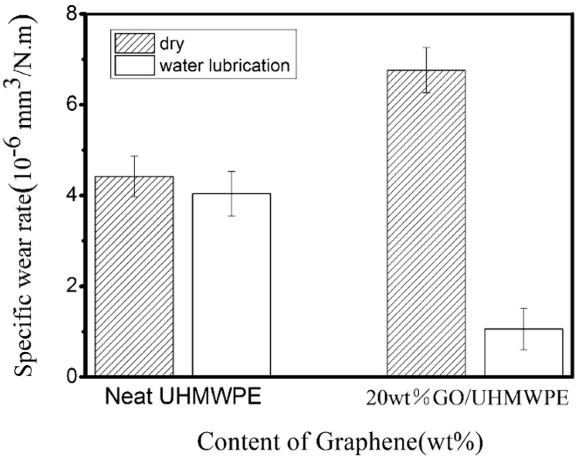

Figure 7. Effect of GO content on wear volume loss of the samples under dry and distilled water lubrication conditions.

120 min under dry condition. It can be seen that the friction coefficient of the GO reinforced UHMWPE composite is increased with the GO weight percentages increasing from 5 to 30%. And the content of 20 wt% GO composite exhibits the best stable friction coefficient than that of the pure UHMWPE or other GO content composites under the same experimental condition.

In addition, the variations of friction coefficient of two typical samples, namely, neat UHMWPE and 20 wt% GO reinforced UHMWPE composite, under different lubrication conditions have been studied, which are shown in Figure 6. Under distilled water lubrication, the friction coefficient of the 20 wt% GO reinforced UHMWPE composite was lower than that of the pure UHMWPE.

Furthermore, wear volume loss is another important indicator to value the frictional resistance of sample. Figure 7 presents the effect of GO content on wear volume loss of the samples under dry and distilled water lubrication conditions. The volume loss under dry sliding was higher than that under distilled water lubrication for each sample, thus, the volume loss of the 20 wt% GO reinforced UHMWPE composite was 4 times lower than the neat UHMWPE under distilled water lubrication.

The effect of GO on mechanical properties of GO/UHMWPE composites was studied. Figure 8(a) shows the tensile strength and Young's modulus of composites with various GO loadings. With increasing GO nanosheets, the tensile strength and Young's modulus of GO/UHMWPE composite obviously increased, the reason might be attributed to the homogeneous dispersion of GO nanosheets in the polymer matrix and strong interfacial interactions between both components. The effect of GO content on hardness of the composites has been studied, which is shown in Figure 8(b). The hardness of composites was gradually increased when GO were added to the matrix. The addition of GO, which have high strength and clash mod-

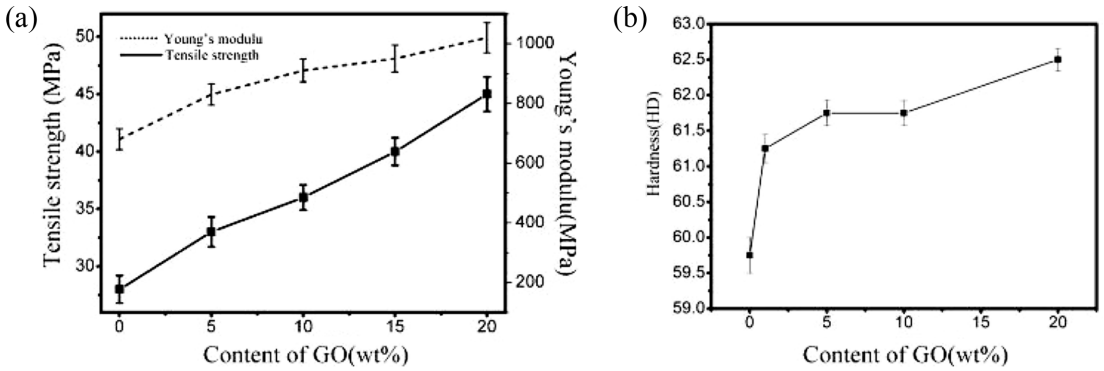

Figure 8. Tensile strength and Young's modulus of UHMWPE composites with various GO loadings (a); hardness variation graphs of GO reinforced UHMWPE composites with the amount of GO changed (b).

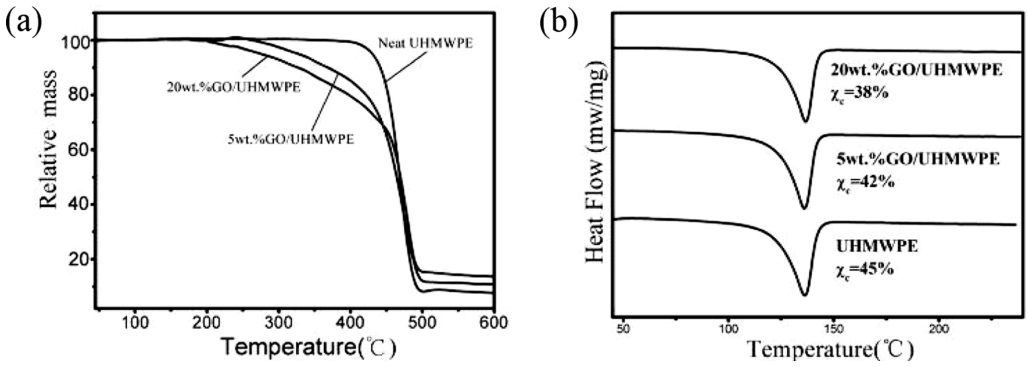

Figure 9. TGA curves of neat UHMWPE and GO/UHMWPE composites (a); the DSC curves of UHMWPE and GO/UHMWPE composites (b).

ulus, contributes to the increase in hardness of the UHMWPE composites.

The thermogravimetric analysis (TGA) is used to investigate the thermal stability of neat UHMWPE and GO/UHMWPE composites (Figure 9(a)), Both neat UHMWPE and GO/UHMWPE composites had the similar decompose curves, but TGA curves (200-400 ºC) of GO/UHMWPE composites were shifted to a lower temperature compared to that of pure UHMWPE, it might be attributed to decompose of GO. Simultaneously, the crystallinity of UHMWPE composites is further demonstrated by differential scanning calorimetry (DSC) measurement, as shown in Figure 9(b). The fully exfoliated and well-dispersed GO nanosheets among the UHMWPE chains, a physical barrier, which could dramatically diminish the crystallinity of UHMWPE matrix.[21]

The worn surfaces of UHMWPE and 20 wt% GO/UHMWPE composite under dry and distilled water lubrication conditions can be seen from the SEM images (Figure 10). The worn surface of UHMWPE composites is quite different for each of friction condition. In dry sliding (Figure 10(a)), because of friction heat softening rolled in the polymer matrix and micro-adhesive wears, worn surface of UHMWPE is more of fibrillar type debris that twine round each other on the worn surface. In the distilled water lubrication conditions, the worn surface of pure UHMWPE is smooth, and only exhibit plow traces along sliding direction due to die surface smooth or indentation of ring surface, which is shown in Figure 10(b). The 20 wt% GO/UHMWPE composite worn surfaces have no microscopic undulation and scratch, either under dry sliding (Figure 10(c)) or distilled water lubrication conditions (Figure 10(d)), but plow traces along sliding direction and some GO nanosheets on the worn surface are draw out and abrade.

From above results, one can see GO nanosheets act very

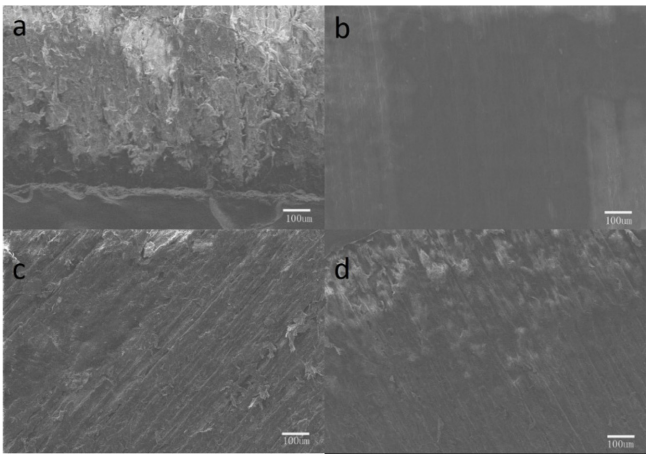

Figure 10. SEM images of worn surfaces of UHMWPE (a and b); 20 wt% GO/UHMWPE composite (c and d) under dry and distilled water lubrication conditions, respectively.

important role on improving wear and mechanical properties of UHMWPE composites. Tribological and hardness tests as shown in Figure 5 and Figure 8 suggested that both applied stress during indentation and frictional stresses transfered to the GO network effectively. Because of high aspect ratio and well-dispersion, GO in the composites provided a large surface area available for interaction between the polymer molecules and GO, which facilitated good load transfer to the GO network. Furthermore, the addition of GO contributes to the increasing of local compressive and shear strength. It is well known that graphite lubrication is environment dependant. The failure of electrical generators in aircrafts flying at high altitude due to the dusting wear regime of carbon brushes has been the starting point of many experimental studies investigating the influence of the gas atmosphere on the friction regime of graphite.[22] Two modes have been observed:[23,24] the dusting fric-

tion mode associated to a high friction coefficient and a high wear rate owing to the rapid disintegration of graphite into a cloud of fine dust-like debris, the low friction mode characterised by a low friction coefficient and a low wear rate. Under dry lubrication conditions, the friction coefficient of the GO reinforced UHMWPE composite is increased with the GO weight percentages increasing from 5 to 20%. The high and erratic friction behavior indicates that the GO/UHMWPE composites are experiencing "dusting" owing to the fibrillar type debris from the UHMWPE and accumulation of dangling bonds generated by GO fractured surfaces. Under distilled water lubrication conditions, the worn surface of GO contains various oxygenated groups and the GO in the composites will fully absorb water. Water has a high surface tension and it is both adhesive and elastic. This property causes water to exist as an extended thin film over solid surface. Water may penetrate into the matrix under water lubrication of GO. Firstly, water is absorbed by capillary action into the voids then stress induced diffusion of water into the void takes place.[25] Mechanistically, microscale swelling of surface layers of GO caused by interaction with water molecules decreases the shear strength and thereby the frictional energy content is brought down. External force induced by sliding causes inter-lamellar insertion of water molecules between the basal planes. In this process, excess amount of water molecules interrupt already weak inter-planar interaction. This process further paves the way for easy shearing due to conversion of sliding to rolling motion under the influence of external force. Chemically, a GO crystal surface is composed of cleavage-faces and edge-faces. The cleavage-face of GO is a low-energy surface that is essentially formed by the basal planes. Water molecules containing hydrogen and oxygen atoms react with the free sites of covalent C–C bond and oxygenated functional groups of GO via adsorption and chemical reactions. This effect is attributed to high mobility of the physisorbed and chemisorbed water molecules that subsequently migrate to high energy edge sites of GO and neutralize dangling covalent bonds that are exposed during sliding. It is therefore the passivation of carbon dangling covalent bonds by adsorption of water that allows composites to maintain a low friction. Because of the reasons mentioned above, the friction coefficient of GO reinforced UHMWPE composites is lower than that of pure UHMWPE under distilled water lubrication conditions, especially, the volume loss of the 20 wt% GO reinforced UHMWPE composite is lower than the neat UHMWPE under distilled water lubrication.

Conclusions

The UHMWPE composites reinforced with GO nanosheets have been prepared by a facile method. The hardness of the GO reinforced UHMWPE composites increases with GO content. Tribological performance studies shows that GO can effectively improve the tribological property of UHMWPE composites. The friction coefficients of the GO reinforced UHMWPE composites are all higher and more stable than that of the pure UHMWPE under dry sliding. The high and erratic friction behavior indicates that the GO/UHMWPE composites are experiencing "dusting" owing to the fibrillar type debris from the UHMWPE and accumulation of dangling bonds generated by GO fractured surfaces. And the friction coefficient of the nanocomposites is lower than that of pure UHMWPE under distilled water lubrication conditions. Super low friction coefficient value and the best wear resistance under distilled water are attributed to water provides passivation of interacting dangling bonds on the sliding surface of GO. The volume loss of the 20 wt% GO reinforced UHMWPE composite is 4 times lower than that of the neat UHMWPE under distilled water lubrication. Thus, the GO/UHMWPE composite materials with good wear resistance under water condition and mechanical properties may have extensive further applications, such as tissue engineering, medical devices and marine engineering.

Acknowledgments: We thank PetroChina Innovation Foundation (2012D-5006-0502) for the financial support of this work.

References

1. M. A. McGee, D. W. Howie, S. D. Neale, D. R. Haynes, and M. J. Pearcy, *Proceedings of the Institution of Mechanical Engineers Part H-Journal of Engineering in Medicine*, **211**, 65 (1997).
2. G. F. Gong, H. Y. Yang, and X. Fu, *Wear*, **256**, 88 (2004).
3. A. Chanda, A. K. Mukhopadhyay, D. Basu, and S. Chatterjee, *Ceram. Int*., **23**, 437 (1997).
4. H. J. Park, S. Y. Kwak, and S. Kwak, *Macromol. Chem. Phys*., **206**, 945 (2005).
5. D. S. Xiong, *Mater. Lett.*, **59**, 175 (2005).
6. K. S. Novoselov, A. K. Geim, S. V. Morozov, D. Jiang, Y. Zhang, S. V. Dubonos, I. V. Grigorieva, and A. A. Firsov, *Science*, **306**, 666 (2004).
7. A. K. Geim and K. S. Novoselov, *Nat. Mater.*, **6**, 183 (2007).
8. M. J. McAllister, J.-L. Li, D. H. Adamson, H. C. Schniepp, A. A. Abdala, J. Liu, M. Herrera-Alonso, D. L. Milius, R. Car, R. K. Prud'homme, and I. A. Aksay, *Chem. Mater.*, **19**, 4396 (2007).

9. C. Lee, X. Wei, J. W. Kysar, and J. Hone, *Science*, **321**, 385 (2008).
10. S. Kwon, J.-H. Ko, K.-J. Jeon, Y.-H. Kim, and J. Y. Park, *Nano Letters*, **12**, 6043 (2012).
11. R. Ansari, S. Ajori, and B. Motevalli, *Superlattice Microst.*, **51**, 274 (2012).
12. O. Penkov, H.-J. Kim, H.-J. Kim, and D.-E. Kim, *Int. J. Precis. Eng. Manu.*, **15**, 577 (2014).
13. C. Yan, K.-S. Kim, S.-K. Lee, S.-H. Bae, B. H. Hong, J.-H. Kim, H.-J. Lee, and J.-H. Ahn, *ACS Nano*, **6**, 2096 (2012).
14. J. Ou, J. Wang, S. Liu, B. Mu, J. Ren, H. Wang, and S. Yang, *Langmuir*, **26**, 15830 (2010).
15. H. Liang, Y. Bu, J. Zhang, Z. Cao, and A. Liang, *ACS Appl. Mater. Interf.*, **5**, 6369 (2013).
16. H. Bai, C. Li, and G. Shi, *Adv. Mater.*, **23**, 1089 (2011).
17. C. Valles, C. Drummond, H. Saadaoui, C. A. Furtado, M. He, O. Roubeau, L. Ortolani, M. Monthioux, and A. Penicaud, *J. Am. Chem. Soc.*, **130**, 15802 (2008).
18. W. S. Hummers and R. E. Offeman, *J. Am. Chem. Soc.*, **80**, 1339 (1958).
19. S. Park, J. An, R. D. Piner, I. Jung, D. Yang, A. Velamakanni, S. T. Nguyen, and R. S. Ruoff, *Chem. Mater.*, **20**, 6592 (2008).
20. A. Lerf, H. He, M. Forster, and J. Klinowski, *J. Phys. Chem. B*, **102**, 4477 (1998).
21. C. Bao, Y. Guo, L. Song, and Y. Hu, *J. Mater. Chem.*, **21**, 13942 (2011).
22. R. H. Savage, *J. Appl. Phys.*, **19**, 1 (1948).
23. J. K. Lancaster and J. R. Pritchard, *J. Phys. D-Appl. Phys.*, **14**, 747 (1981).
24. B. K. Yen, *Wear*, **192**, 208 (1996).
25. H.-J. Song, Z.-Z. Zhang, and Z.-Z. Luo, *Surf. Coat. Technol.*, **201**, 2760 (2006).